Fundamental Analysis for Cooperative Reception Scheme using Mobile Aerial Base Stations in Wireless Sensor Networks

Shintaro Mori

Department of Electronics Engineering and Computer Science
Fukuoka University
8-19-1, Nanakuma, Jonan-ku, Fukuoka 814-0180, Japan
e-mail: smori@fukuoka-u.ac.jp

Abstract—**The Internet of Things (IoT) and emerging wireless sensor networks (WSNs) have been widely adopted in various fields and are attracting attention. In addition, low power wide area (LPWA) technologies have shown great advances and are applicable to IoT and WSN solutions. LPWA-based WSNs are effective when wireless data transmissions are sent at long periodic time intervals. However, vast amounts of forwarding data cannot be handled due to collision and congestion. To overcome this technical issue, in this paper, we propose a novel cooperative (hybrid) reception scheme using mobile aerial base stations (MBSs) mounted on unmanned aerial vehicles (UAVs). Moreover, we fundamentally demonstrate that the proposed mechanism can improve frame-reception probability based on exhaustive computer simulation. As a result, the proposed scheme achieves up to 8.32-times better performance than a comparable scheme without using MBSs.**

Keywords-wireless sensor network; unmanned aerial vehicle; low power wide area network; mobile aerial base station

I. INTRODUCTION

As one of the fastest growing technologies, the Internet of Things (IoT) promises to revolutionize the way we live and work, and advanced wireless sensor network (WSN) systems have become technically easy to build in the past several years. With this background, there is great potential to meet the huge demands for IoT systems. However, major challenges remain, such as the tradeoff between low energy consumption and extensive wireless area coverage. Notably, typical sensor node (SN) devices have become tiny and cheap, including resource-constrained processing modules and small batteries with a limited energy budget [1].

To construct a long-lived WSN system, most studies adopt such measures as cooperative communication techniques, network coding schemes, clustering mechanisms, and so on. On the other hand, other solutions require the emergence of a new-type of architecture. Low power wide area (LPWA) network [2][3] techniques represent a novel wireless network paradigm that complements traditional cellular and short-range wireless communications in addressing the diverse requirements of IoT applications. These techniques include, for example, long-range wide area network (LoRa WAN) [4], Sigfox [5], and narrowband IoT (NB-IoT) [6].

A variety of LPWA technologies can provide the means to sense and collect environmental data anywhere and anytime: several kilometers-order coverage areas, narrowband channel occupancy, periodical transmission, and the unsophisticated physical (PHY) and media access control (MAC) protocols. In fact, at the PHY layer, a low-bit-rate and noise-robust modulation scheme, such as the binary phase shift keying (BPSK) method and the (Gaussian) frequency shift keying ((G)FSK) method, is typically used. In addition, LPWA systems commonly use the radio frequency of sub-GHz bands, such as 915 MHz for the USA, 868 MHz for the EU, and 920 MHz for Japan. Furthermore, at the MAC layer, a pure-ALOHA procedure is commonly adopted, where data are sent if a node has data to send, collisions occur when any new data are released while any node is transmitting, and both of these data are lost. To investigate the effectiveness of LPWA systems, Adelantado et al. [7] surveyed the capabilities and limitations of LoRa WAN systems. Bor et al. [8] experimentally demonstrated that the current LPWA scheme could not provide sufficient performance for typical smart city deployment, that is, 120 nodes per 0.038 km^2. At the same time, conventional LPWA-based WSN systems can operate effectively even if the PHY and MAC protocols are constructed by a simple procedure that only requires data transmitted at a sufficiently long-interval for uploading requests. However, in the near-future, we cannot expect vast amounts of forwarding data to be handled based on a traditional scheme due to collision and congestion.

In this paper, as a way to overcome this technical issue, we propose a novel cooperative (hybrid) reception scheme by using mobile aerial base stations (MBSs) mounted on unmanned aerial vehicles (UAVs), such as drones and small planes [9][10]. The goal of this paper is to present a fundamental analysis technique for improving the probability of frame reception. Its performance for UAV-mounted MBSs in LPWA-based WSNs is still unknown. Nevertheless, our study shows significant results from our preliminary analysis.

Regarding related studies, Li and Cai [11] proposed an MBS-based offloading mechanism for solving the problem of increased traffic volume in heterogeneous cellular networks. Sharma et al. [12] investigated the same concept, but they proposed a user-driven MBS deployment scheme. For the MBS placement's and UAV trajectory's decision formula, Lyu et al. [13] proposed a placement algorithm to minimize the number of MBSs needed to provide wireless coverage. Furthermore, Mozaffari et al. [14] and Alzenad [15] expanded the technique of Lyu et al. [13] for the 3D location scenario. On the other hand, another study of Mozaffari et al. [16] investigated a topic similar to that taken up in this paper. In that work, they did not take into account the MAC protocol design, and their simulation was conducted under a traditional
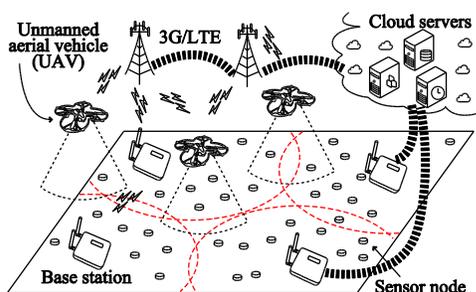
Figure 1. Network model of proposed scheme

(a) Placement of SNs, BSs, and UAVs

Typical transmission:

Collision occurring (hotspot):

Long-distance data transmission (cell-edge):

Conventional scheme   Proposed scheme

(b) Packet processing scenario at MAC layer

Figure 2. Typical scenarios in which proposed scheme operates

WSN usage, with the radio frequency set to the 2-GHz industry science medical (ISM) band and 500 SNs distributed over a 1 km^2 area. — In the proposed scheme, the radio frequency is set to 920 MHz (i.e., a sub-GHz band) and up to 500,000 SNs are distributed.

The remainder of this paper is organized as follows. Section II describes the proposed scheme. Section III provides computer simulation result. Finally, in Section IV, we summarize our findings and conclude the paper.

II.   PROPOSED SCHEME

In the proposed scheme (Figure 1), the SNs periodically transmit the sensing data, which their neighbor base stations (BSs) receive and forward to the cloud servers. In addition, the UAV flies at the edge of the cell coverage area, which offers a poor radio-propagation environment, as well as the gap area outside the BSs' coverage range and the hotspot area where the sensing data are generated at a greater rate than in the surrounding area. We assume that BSs, MBSs, and cloud servers are ideally connected with each other through mobile cellular networks, and we focus on the wireless links between SNs and BSs and between SNs and MBSs. Moreover, the BSs and MBSs are provided with sufficient power supply, while the SNs have a strictly limited battery capacity, since the battery exchange cost is non-remunerative and relatively expensive due to use of cheap hardware devices. Therefore, ensuring sophisticated and intelligent transmission control in the SN device is not realistic. In other words, the proposed concept using UAV-mounted MBSs that cooperatively operate with legacy BSs at the receiver side might be a reasonable idea.

In the rest of this section, we explain how to improve the frame-reception probability by using the proposed mechanism. As shown in Figure 2 (a), we assume that three SN devices ($\mathbb{A}$, $\mathbb{B}$, and $\mathbb{C}$) are deployed within the BS's coverage cell, where $\mathbb{A}$ and $\mathbb{B}$ are located at the same distance from the BS while $\mathbb{C}$ is located in the cell-edge area at a farther distance, and that the UAV aviates in the border region between adjacent cells. In this case, as shown in Figure 2 (b), we assume three MAC procedure scenarios: typical transmission, collision occurring in the hotspot, and long-distance data transmission in the cell-edge region. We found that the proposed scheme can work effectively in the latter two scenarios.
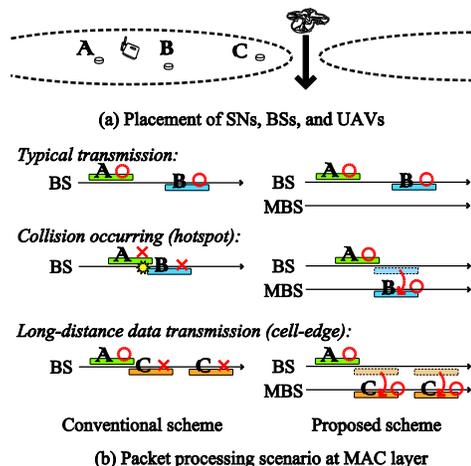
For the typical transmission and collision occurring in the hotspot scenario, the conventional LPWA-based WSN system works without causing collisions due to its sparse channel allocation requests. According to the increased SN, in Figure 2 (b), $\mathbb{B}$ tries to send its frame while $\mathbb{A}$ transmits its own frame; consequently, both $\mathbb{A}$'s frame and $\mathbb{B}$'s frame are lost due to the pure-ALOHA feature. In this situation, their frames should be retransmitted after random back-off time, which might contribute to additional frame collisions. In the proposed scheme, if the MBS's channel were by chance not busy and $\mathbb{B}$'s frame could be moved from the BS to the MBS, both frames might be successfully transferred. Here, among $\mathbb{A}$, $\mathbb{B}$, BSs, and MBSs, the wireless links are selected in the shared radio frequency band. On the other hand, $\mathbb{B}$ sends its frame via an exclusive radio channel different from that for $\mathbb{A}$'s frame. Hence, we can assume that $\mathbb{A}$ and $\mathbb{B}$ can be communicated with BSs and MBSs without interference.

For long-distance data transmission in the cell-edge scenario, $\mathbb{C}$'s frame request does not fatally affect $\mathbb{A}$'s frame transmission. In other words, $\mathbb{C}$'s frame is inevitably lost regardless of the scenario. In the proposed scheme, since MBSs can collect the cell-edge node's frame, such as $\mathbb{C}$'s frame, the overall frame-reception probability can be improved.

The proposed scheme does not check the availability of the MBS channel in order to avoid system complexity for the SN device; instead, we consider compatibility with the traditional LPWA's MAC protocol like the pure-ALOHA procedure. On the other hand, to further improve throughput, we should introduce an intelligent frequency-sharing mechanism for use among SNs, BSs, and MBSs: This remains our important future work.

III.   COMPUTER SIMULATION

In this section, we demonstrate the fundamental performance of our proposed mechanism, i.e., the ability to improve frame-reception probability, using an exhaustively prepared computer simulator implemented in C++ language.
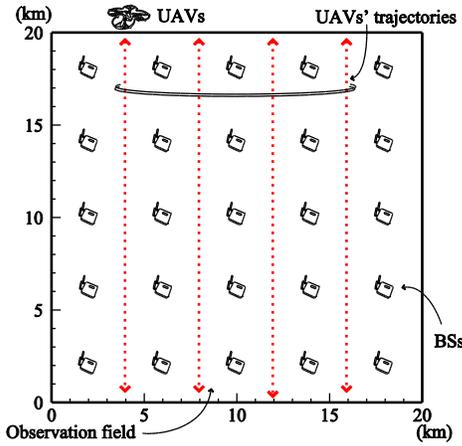
Figure 3. Deployment and trajectory of SNs, BSs, and MBSs (UAVs)

A. Simulation model

In the computer simulation model (Figure 3), BSs are deployed in the lattice (grid) pattern, MBSs (on UAVs) aviate between BSs, and SNs are randomly scattered over the surface of the observation area. We assume that the UAVs can aviate at all times by changing to alternate aircraft along the given fixed trajectory (red line in Figure 3). The detailed simulation parameters are summarized in Table I. Individual SNs generate the sensing data with equal frequency, and the parameter settings of the MAC layer are set based on the Japanese LoRa WAN specifications [17]. For frame reachability, we calculate the received signal-to-noise ratio (SNR) based on the manner described in Section III.B, and we compare the obtained SNR with the required SNR based on the manner given in Section III.C.

B. Radio propagation model

In our computer simulation, we calculated the receiver side's signal strength based on the distance between the transmitter side and the receiver side. According to the typical link budget formula [18], the received signal strength in decibel can be calculated as

$$P_{RX} = P_{TX} - L_{TX} + G_{TX} - L_P(d) + G_{RX} - L_{RX} , \quad (1)$$

where, at the transmitter and receiver sides, respectively, P_{TX} and P_{RX} denote electrical radio powers, L_{TX} and L_{RX} denote electrical power loss in the physical circuit and impedance mismatching, and G_{TX} and G_{RX} denote antenna gains.

In (1), $L_P(d)$ denotes radio propagation loss, and it can generally be represented as

$$L_P(d) = \alpha + 10 \cdot \beta \cdot \log_{10}(d) + S , \quad (2)$$

where d denotes the distance between terminals, S denotes shadowing variation, and both α and β are given by individual radio propagation models. In this paper, we select the model of Erceg et al. [19] for the link between SNs and

TABLE I. SIMULATION PARAMETERS

Terms		Values
Observation area		Square, 20 km × 20 km
Sensor node	Number of SNs	1,000–500,000
	Trans. interval	1,200 s (= 20 min.)
Base station	Number of BSs	25
	Antenna height	h_{BS} = 50.0 m
UAV	Number of aircrafts	20
	Altitude	120 m
	Velocity	5.56 m/s (= 20 km/hr.)
MAC layer	Protocol	pure ALOHA
	Number of channels	3
	Transmission time	4 s
	Max retrans. num.	3
	Max back-off time	30 s
	Frame length	ℓ = 50 byte (= 400 bit)
	Req. frame error prob.	P_e = 0.5 %, 1 %, 2 %, 5 %
PHY layer	Modulation method	BPSK, Binary FSK
	Error control coding	NA
	Radio frequency	920 MHz (λ = 0.326 m)
	Channel model	Rayleigh fading
	Radio-propagation model	Erceg's model (SN–BS), Amorim's model (SN–UAV)
Parameters of Erceg's model (Flat surface ground, light tree density)		a = 3.6, b = 0.005, c = 20.0, ε = 0.59, d_0 = 100 m, μ_S = 8.2, σ_S = 1.6
Parameters of Amorim's model		σ_S = 3.4
Link-budget constant parameters	Transmission power	P_{TX} = 13.0 dBm (20 mW)
	Antenna gain	G_{TX} = 0 dBi, G_{RX} = 3.53 dBi
	Circuit loss	$L_{TX} = L_{RX}$ = 0 dB

BSs and the model of Amorim et al. [20] for the link between SNs and MBSs. These models were formulated based on experimental measurements, and we separately used them by considering the difference between line-of-sight (LOS) propagation (for SNs-MBSs) and non-LOS (NLOS) propagation (for SNs-BSs).

Consequently, the parameters of α, β, and S in (2) can be characterized as follows:

Erceg et al.'s model: S is a random variable with normal distribution of $\mathcal{N}(\mu_S, \sigma_S^2)$, and both α and β can be calculated as

$$\begin{cases} \alpha = 20 \log_{10}(4\pi d_0/\lambda) , \\ \beta = (a - b h_{BS} + c/h_{BS}) + \varepsilon \cdot z , \end{cases} \quad (3)$$

where h_{BS} denotes the antenna height of BS, λ denotes the carrier radio wavelength, and a, b, c, d, and ε denote the constant values depending on the surrounding environment [19]. In addition, z is a random variable with a normal distribution of $\mathcal{N}(0, 1)$.

Amorim's model: S is a random variable with normal distribution of $\mathcal{N}(0, \sigma_S^2)$, and both α and β are given by $\alpha = 35.3$ and $\beta = 2.0$, depending on the UAV altitude [20].
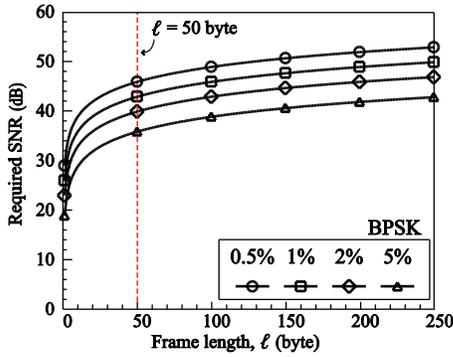
Figure 4. Frame length, ℓ, versus required SNR for BPSK method
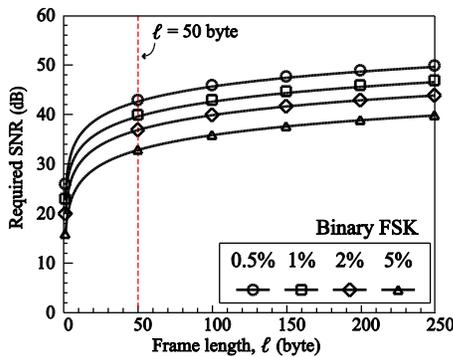
Figure 5. Frame length, ℓ, versus required SNR for Binary FSK method

C. Required SNR calculation

In this paper, we consider the BPSK method and Binary FSK method as the modulation scheme. In general, the bit error probability, p_b, under the Rayleigh fading environment can be theoretically calculated [18] as follows:

$$
\begin{cases}
p_b = \left[1 - \sqrt{\gamma/(1+\gamma)}\,\right]/2 & \text{(BPSK)}, \\
p_b = \left[1 - \sqrt{\gamma/(2+\gamma)}\,\right]/2 & \text{(Binary FSK)},
\end{cases}
\tag{4}
$$

where γ denotes SNR, and the relationship between γ and P_{RX} is given by

$$
\gamma = P_{RX}/\kappa\tau_o , \tag{5}
$$

where κ (= 4.0×10^{-21} W/Hz) denotes Boltzmann's constant value and τ_o (K) denotes the system device's absolute temperature. Therefore, by letting ℓ (bit) denote frame length, we can calculate the frame error probability, p_e, using (4) as

$$
p_e = 1 - (1 - p_b)^\ell . \tag{6}
$$

Figures 4 and 5 show the calculation results for the frame length, ℓ, versus the required SNR when the p_e values are
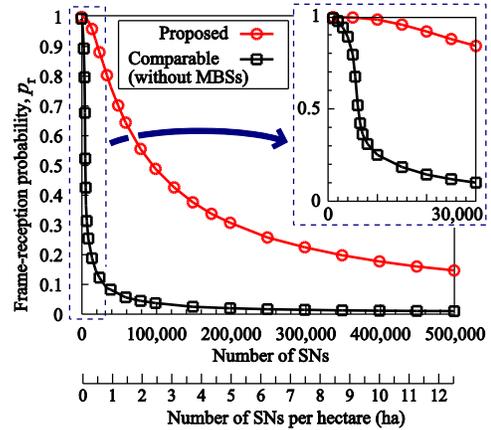
Figure 6. Number of SNs versus frame-reception probability

0.5%, 1%, 2%, and 5% for the BPSK and Binary FSK methods, respectively, based on the above procedure.

D. Numerical result

When the frame error probability is 0.5% and $\ell = 50$ bytes (i.e., the maximum LoRa frame length transmitted in the airtime allowed by Japanese regulations [17]), based on Figures 4 and 5, we can obtain the required received power as -126 dBm and -129 dBm for the BPSK and Binary FSK methods, respectively. In (5), the required P_{RX} can be obtained as 43 dBm and 46 dBm based on Figures 4 and 5, and in the general condition, $\kappa\tau_o$ is given as -172 dBm.

Figure 6 shows the number of SNs (and number of SNs per hectare) versus frame-reception probability, p_r, which is calculated as

$$
p_r = N_r / N_{all} , \tag{7}
$$

where N_r and N_{all} denote the number of successfully received frames and the number of all generated frames, respectively. Consequently, in the comparable scheme without using MBSs, the frame-reception probability was dramatically degraded. This is because frame collisions and retransmissions significantly increased as they exceeded the multiple access capability of the pure-ALOHA method. We believe this phenomenon led to the same conclusion reached in Adelantado et al. [7] and C. Bor et al. [8].

On the other hand, the proposed scheme could reduce the worse degradation in the frame-reception probability curve, even if the SNs increased. When the required frame-reception probabilities were 0.9, 0.8, and 0.5, the proposed scheme with MBSs could increase the number of SNs (and per hecare) by 5.77, 7.00, and 15.8 times, respectively, compared to the scheme without MBSs, while still keeping the same farme reception rate in the end. Finally, the proposed scheme achieved up to 8.32 times better performance in frame-reception probability than the comparable scheme.

IV. CONCLUSION

In this paper, we proposed a novel cooperative (hybrid) reception scheme using UAV-mounted mobile aerial base stations for LPWA-based WSNs. Computer simulation demonstrated that the proposed scheme achieved up to 8.32 times better performance than a comparable scheme without using MBSs in terms of the frame-reception probability. In future work, we should consider such issues as an extended receiver-side cooperation mechanism, MBS placement and algorithms for detetmining the UAV's flight path and aircraft selection.

REFERENCES

[1] G. Anastasi, M. Conti, M. Di Francesco, and A. Passarella, "Energy Conservation in Wireless Sensor Networks: A Survey," *Ad Hoc Networks*, vol. 7, no. 3, pp. 537–568, May 2009.

[2] U. Raza, P. Kulkarni, and M. Sooriyabandara, "Low Power Wide Area Networks: An Overview," *IEEE Commun. Surveys & Tutorials*, vol. 19, no. 2, pp. 855–873, Second-quarter 2017.

[3] H. Wang and A. O. Fapojuwo, "Survey of Enabling Technologies of Low Power and Long Range Machine-to-Machine Communications," *IEEE Commun. Surveys & Tutorials*, vol. 19, no. 4, pp. 2621–2639, Fourth-quarter 2017.

[4] LoRa, https://www.lora-alliance.org/ [retrieved: Mar. 2018].

[5] Sigfox, https://www.sigfox.com/ [retrieved: Mar. 2018].

[6] Y. P. E. Wan et al., "A Primer on 3GPP Narrowband Internet of Things," *IEEE Commun. Mag.*, vol. 55, no. 3, pp. 117–123, Mar. 2017.

[7] F. Adelantado et al., "Understanding the Limits of LoRaWAN," *IEEE Commun. Mag.*, vol. 55, no. 9, pp. 34–40, Sept. 2017.

[8] M. C. Bor, U. Roedig, T. Voigt, and J. M. Alonso, "Do LoRa Low-Power Wide-Area Networks Scale," *Proc. the 19th Int. Conf. Modeling, Analysis, and Simulation of Wireless and Mobile Syst. (MSWiM'16)*, Nov. 2016, pp. 59–67, doi: 10.1145/2988287.2989163.

[9] A. T. Erman, L. V. Hoesel, P. Havinga, and J. Wu, "Enabling Mobility in Heterogeneous Wireless Sensor Networks Cooperating with UAVs for Mission-critical Management," *IEEE Wireless Commun.*, vol. 15, no. 6, pp. 38–46, Dec. 2008.

[10] Y. Zeng, R. Zhang, and T. J. Lim, "Wireless Communications with Unmanned Aerial Vehicles: Opportunities and Challenges," *IEEE Commun. Mag.*, vol. 54, no. 5, pp. 36–42, May 2016.

[11] Y. Li and L. Cai, "UAV-assisted Dynamic Coverage in Heterogeneous Cellular System," *IEEE Network*, vol. 31, no. 4, pp. 56–61, July–Aug. 2017.

[12] V. Sharma, M. Bennis, and R. Kumar, "UAV-assisted Heterogeneous Networks for Capacity Enhancement," *IEEE Commun. Lett.*, vol. 20, no. 6, pp. 1207–1210, June 2016.

[13] J. Lyu, Y. Zeng, R. Zhang, and T. J. Lim, "Placement Optimization of UAV-mounted Mobile Base Stations," *IEEE Commun. Lett.*, vol. 21, no. 3, pp. 604–607, Mar. 2017.

[14] M. Mozaffari, W. Saad, M. Bennis, and M. Debbah, "Efficient Deployment of Multiple Unmanned Aerial Vehicles for Optimal Wireless Coverage," *IEEE Commun. Lett.*, vol. 20, no. 8, pp. 1647–1650, Aug. 2016.

[15] M. Alzenad, A. El-Keyi, F. Lagum, and H. Yanikomeroglu, "3-D Placement of an Unmanned Aerial Vehicle Base Station (UAV-BS) for Energy-Efficient Maximal Coverage," *IEEE Wireless Commun. Lett.*, vol. 6, no. 4, pp. 434–437, Aug. 2017.

[16] M. Mozaffari, W. Saad, M. Bennis, and M. Debbah, "Mobile Unmanned Aerial Vehicles (UAVs) for Energy-Efficient Internet of Things Communications," *IEEE Trans. Wireless Commun.*, vol. 16, no. 11, pp. 7574–7589, Nov. 2017.

[17] ARIB STD-T108, https://www.arib.or.jp/english/ [retrived: Mar. 2018].

[18] J. G. Proakis, *Digital Communications*, McGraw-Hill, Jan. 2008.

[19] V. Erceg et al, "An Empirically Based Path Loss Model for Wireless Channels in Suburban Environment," *IEEE J. Sel. Areas in Commun.*, vol. 17, no. 7, pp. 1205–1211, July 1999.

[20] R. Amorim et al., "Radio Channel Modeling for UAV Communication Over Cellular Networks," *IEEE Wireless Commun. Lett.*, vol. 6, no. 4, pp. 514–517, Aug. 2017.